



Improvement of catalytic activity over Cu–Fe modified Al-rich Beta catalyst for the selective catalytic reduction of NO_x with NH₃



Li Xu ^a, Chuan Shi ^{a,*}, Bingbing Chen ^a, Qi Zhao ^a, Yongjun Zhu ^a, Hermann Gies ^b, Feng-Shou Xiao ^c, Dirk De Vos ^d, Toshiyuki Yokoi ^e, Xinhe Bao ^f, Ute Kolb ^g, Mathias Feyen ^h, Stefan Maurer ^h, Ahmad Moini ⁱ, Ulrich Müller ^h, Weiping Zhang ^{a,**}

^a State Key Laboratory of Fine Chemicals, School of Chemistry, Dalian University of Technology, Dalian, 116024, China

^b Institute für Geologie, Mineralogie und Geophysik, Ruhr-Universität Bochum, Germany

^c Department of Chemistry, Zhejiang University, Hangzhou, 310028, China

^d Centre for Surface Chemistry and Catalysis, K. U. Leuven, Leuven, Belgium

^e Chemical Resources Laboratory, Tokyo Institute of Technology, Yokohama, Japan

^f State Key Laboratory of Catalysis, Dalian Institute of Chemical Physics, Dalian, 116023, China

^g Institut für Physikalische Chemie, Johannes Gutenberg-Universität Mainz, 55128, Mainz, Germany

^h BASF SE, Process Research and Chemical Engineering, 67056, Ludwigshafen, Germany

ⁱ BASF Corporation, Catalysts LLC, Iselin, NJ, 08830, USA

ARTICLE INFO

Article history:

Received 4 March 2016

Received in revised form

28 May 2016

Accepted 31 August 2016

Available online 31 August 2016

Keywords:

Al-rich Beta

Cu–Fe-Beta

NH₃-SCR

Synergistic effect

Sulfur resistance

ABSTRACT

Copper and iron bimetal modified Al-rich Beta zeolites from template-free synthesis were prepared for selective catalytic reduction (SCR) of NO_x with NH₃ in exhaust gas streams. Comparing to the Cu-based and Fe-based mono-component Beta catalysts, Cu(3.0)-Fe(1.3)-Beta bi-component catalyst shows better low-temperature activity and wider reaction-temperature window. Over 80% of NO conversion can be achieved at the temperature region of 125–500 °C. Due to the synergistic effect of copper and iron evidenced by XRD, UV–Vis–NIR, EPR and XPS measurements, the dispersion state of active components as well as the ratio of Cu²⁺/Cu⁺ and Fe³⁺/Fe²⁺ were improved over Cu(3.0)-Fe(1.3)-Beta. Isolated Cu²⁺ and Fe³⁺ ions which located at the exchange sites could be the active species at the low-temperature region, while FeO_x cluster species may be more important to the high-temperature activity. During the test of sulfur resistance, Fe-containing samples including Cu(3.0)-Fe(1.3)-Beta and Fe(2.7)-Beta-4 present better performance compared to Cu(4.1)-Beta-4. Deactivation of Cu-based catalyst is attributed to the easier deposition of sulfates over the surface according to the results of TGA coupled with TPD experiments.

© 2016 Elsevier Inc. All rights reserved.

1. Introduction

Selective catalytic reduction (SCR) of nitric oxide with ammonia/urea is the technology widely employed for the control of nitrogen oxides (NO_x) from lean-burn engines operated with excess air. Copper and iron based zeolites catalysts (mostly Cu-ZSM-5 and Fe-ZSM-5) are known to be effective for the NH₃-SCR process [1–5]. Generally, Cu-containing zeolites show better performances at lower temperatures below 300 °C [6]. At above 350 °C, however,

NO_x conversion decreases rapidly. Interestingly, Fe-containing catalysts present better activities at higher temperatures. To achieve wider reaction-temperature window, combination of copper and iron components for the fabrication of multiple metal-containing zeolite catalysts seems to be possible. Actually, several attempts have been made in recent years. Kucherov et al. suggested that for Fe-Beta catalyst, active Fe³⁺ occupies only a fraction of cationic positions in the Beta matrix [7]. Thus, the non-occupied positions can host other metals for the appearance of new properties. Through the replacement of Fe³⁺ in cationic positions by Cu²⁺ by stepwise impregnation method, they found that the de-NO_x activity increases in low-temperature region together with significant loss at higher temperatures. By combination of Cu-SSZ-13 and Fe-ZSM-5 catalysts in the form of two wash coat layers, Metkar et al.

* Corresponding author.

** Corresponding author.

E-mail addresses: chuanshi@dlut.edu.cn (C. Shi), wzhang@dlut.edu.cn (W. Zhang).

obtained the wider NO_x conversion temperature window [8]. They suggested that at low temperatures, the Cu-zeolite bottom layer is highly active. While at higher temperatures, the Fe-zeolite top layer is more selective. Sultana et al. reported a Cu-Fe/ZSM-5 catalyst prepared by subsequent ion-exchange method, which showed higher NO_x conversion compared with Fe-ZSM-5 or Cu-ZSM-5 [9]. They contributed it to the facile reduction of metal species. Through the two-step ion-exchange method, Yang et al. reported a Cu-Fe-SSZ-13 catalyst with best NO_x conversion activity at 150–650 °C and is hydrothermally stable [10]. They contributed the high activity at 150 °C to the fact that Fe³⁺ is hosted in zeolite structures in the vicinity of Cu²⁺.

In our previous work, we reported the superior activity of Cu exchanged Al-rich Beta zeolite from the template-free synthesis (Si/Al ratio ≈ 4) for low-temperature NH₃-SCR compared with the conventional one from the organotemplate synthesis (Si/Al ratio ≈ 19) [11]. We found that Cu-based zeolites could gradually lose its activity at higher temperatures. On the other hand, the SO₂ resistance ability of Cu-zeolites is known to be very poor. Thus, in this paper we aimed to develop a high-efficiency SCR catalyst with wider reaction-temperature window and better SO₂ resistance ability by the introduction of Fe component to the Cu exchanged Al-rich Beta catalyst, which is denoted as Cu-Fe-Beta-4. Herein, the excellent catalytic performances of Cu-Fe-Beta-4 bimetallic zeolite for NH₃-SCR have been demonstrated. Its microstructure characterizations are compared with the Cu-Beta-4 and Fe-Beta-4 single metal-containing zeolite. Correlating the states of active components with the catalytic behavior, the synergistic effect of Cu and Fe components is also identified.

2. Experimental

2.1. Catalyst preparation

Na-Beta zeolite synthesized without organotemplate was obtained from BASF, Germany [12]. The framework Si/Al ratio is about 4.6 as evidenced by our previous ²⁹Si MAS NMR measurement [13]. Before the employment, Na-Beta-4 experienced the conventional ion-exchanged process to its NH₄-type due to the improved NH₃-SCR activity of Fe-containing Beta zeolite from its NH₄-form (Fig. S1). On the basis of NH₄-Beta-4, copper was introduced by the ion-exchanged method with the (CH₃COO)₂Cu aqueous solution. In detail, 1 g of NH₄-Beta-4 was added to 100 ml (CH₃COO)₂Cu aqueous solution of 0.04, 0.06 and 0.08 mol/L, respectively, with stirring at 40 °C for 2 h. After this exchange process, the zeolite slurries were filtered, washed with deionized water and dried at 110 °C for 6 h. The obtained materials were then calcined in muffle oven at 500 °C for 4 h. Iron was then introduced by incipient wetness impregnation with the solution of ferrocene in toluene. 1 g of Cu-Beta-4 was slurried with 1.1 g of toluene containing related amount of ferrocene and placed at room temperature for 48 h. Subsequently, the resulted samples were calcined in air at 500 °C for 2 h. The catalysts were denoted as Cu(m)-Fe(n)-Beta, where m (wt%) and n (wt%) stands for the Cu and Fe content determined by ICP. For comparison, Cu(m)-Beta-4 and Fe(n)-Beta-4 catalysts were also prepared by the identical ion-exchanged process and incipient wetness impregnation, respectively.

2.2. Catalyst characterization

The powder X-ray diffraction (XRD) experiments were performed on a X-ray diffractometer (Rigaku D-Max Rotaflex) using Cu K α radiation ($\lambda = 1.5404 \text{ \AA}$) in a 2θ range of 5–60°.

UV–Vis–NIR diffuse reflectance spectra (UV–Vis–NIR DRS) were recorded in the range of 190–1200 nm on an Agilent Cary-5000 spectrometer.

Electron paramagnetic resonance (EPR) measurements were carried out at –196 °C using a Bruker (A200–9.5/12) spectrometer operating at the X band (~9.8 GHz). The magnetic field was modulated at 100 kHz and the g value was determined from precise frequency and magnetic field values.

The surface chemical states of the samples were examined by X-ray photoelectron spectroscopy (XPS, ESCALAB250 Thermo VG, USA) using an Al K α X-ray source (1486.6 eV) operated at 15 kV and 300 W. Sample charging during the measurements was compensated by an electron flood gun. The XPS data from the regions related to the Cu 2p and/or Fe 2p core levels were recorded. The binding energy was calibrated internally by the carbon deposit C 1s binding energy (BE) at 284.6 eV.

Thermogravimetric analysis (TGA) was carried out on a Q50 TG system (TA, USA) to identify the deposited species formed on the catalytic surface. The sulfated samples were heated from room temperature to 800 °C at 10 °C/min with flowing N₂ (100 ml/min).

Temperature-programmed desorption (TPD) experiment was carried out using an online mass spectrometer (MS, Omini-star, GSD-300) to detect the effluent gases. The sulfated sample was heated to 800 °C with a temperature ramp at a rate of 10 °C/min in Ar stream. MS spectra were recorded with masses characteristic of SO₂ (32, 64), NH₃ (17, 15), N₂ (28), H₂O (17, 18).

2.3. Catalytic tests

The SCR activity measurements were carried out in a fixed-bed quartz reactor (i.e. 6 mm) with the reactant gas mixture containing 500 ppm NO, 500 ppm NH₃, 10% O₂, 2% H₂O (when used), 100 ppm SO₂ (when used) and balance N₂. The total flow rate was 400 ml/min, corresponding to a gas hourly space velocity (GHSV) of about 80,000 h⁻¹. NO, NO₂, NO_x (=NO + NO₂), NH₃ and N₂O contents were monitored continuously using a NO_x analyzer (ML9841AS, Monitor, USA) and NH₃/N₂O analyzer (SickMaihak, Germany), respectively. To avoid errors caused by the conversion of ammonia in the analyzer, an ammonia trap containing phosphoric acid solution was installed upstream. All data were obtained when the SCR reaction reached a steady state at each temperature.

3. Results

3.1. Catalytic activity

3.1.1. Influence of copper and iron contents

Fig. 1 shows the NH₃-SCR activities of copper and iron bimetallic Beta catalysts with various Cu and Fe contents. It can be found that Cu(3.0)-Fe(1.3)-Beta shows the best low-temperature activity. Nearly 85% of NO conversion can be achieved at the temperature as low as 125 °C, and it can reach about 100% NO conversion at 150 °C. While at the high-temperature region (350–550 °C), the conversion shows a gradual decrease. However, it exhibits 78% of NO conversion even at 550 °C, indicating the relative stable high-temperature activity. With Fe concentration increases from 1.3 to 2.2%, no obvious changes appear for Cu(2.8)-Fe(2.2)-Beta at the high-temperature region. While at 125 °C, the NO conversion decreases to 70%, indicating that the excessive introduction of Fe has a negative effect on the low temperature activity of the catalyst. With further increase of Cu content to 4.0% while keeping Fe content at a lower level of 0.6%, the catalyst shows the poorest high temperature activities, which should be related to its lowest Fe content. Meanwhile the NO conversion at low temperature (125 °C) is not enhanced with increasing Cu loading from ca. 3.0–4.0%, indicating

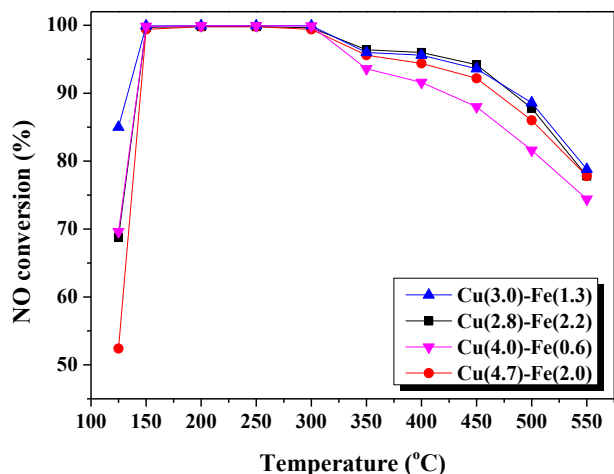


Fig. 1. SCR performance of bi-component Beta catalysts with various Cu, and Fe concentrations. Reaction conditions: 500 ppm NO, 500 ppm NH₃, 10% O₂, and N₂ balance; GHSV: 80,000 h⁻¹.

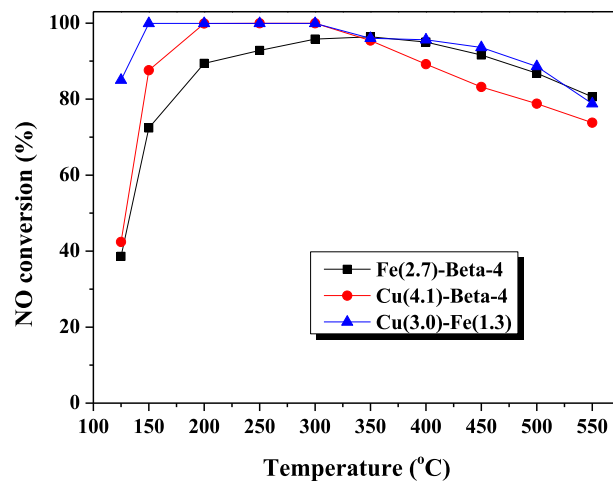
that a proper Cu content is essential for the best activity, which is in accordance with our previous result [11]. With further increase of Cu content from 2.8 to 4.7% and Fe content from 0.6 to 2.0%, the NO conversion decreases to ca. 53% at 125 °C. At higher temperatures, Cu(4.7)-Fe(2.0)-Beta presents similar performance with Cu(2.8)-Fe(2.2)-Beta. According to the above results, it is reasonable to suppose that the bimetallic Beta catalysts with appropriate Cu and Fe contents would present better catalytic behavior.

3.1.2. Influence of active components

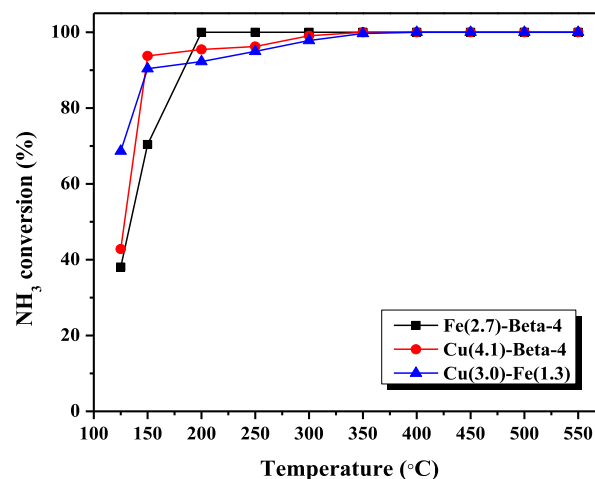
NO conversion over Cu, Fe and Cu-Fe metal containing Beta catalysts are presented in Fig. 2. For Fe(2.7)-Beta-4 catalyst, NO conversion is less than 40% at the low temperature of 125 °C. With increasing temperature, NO conversion increases and reaches nearly 72% at 150 °C. At 200 °C, the catalyst reaches ~90% of NO conversion. Upon the reaction temperature above 400 °C, the activity decreases. Fortunately, about 80% of NO conversion could be achieved at 550 °C. For Cu(4.1)-Beta-4 catalyst, NO conversion is ca. 42% at 125 °C. With increase of temperature, NO conversion increases to 88% at 150 °C, and reaches 100% at 200 °C. At the temperature above 350 °C, the activity in NO conversion shows sharp decrease, which is below 80% at 500 °C. Comparing the activities of mono-component Beta catalysts, it can be found that Cu-based catalyst appears better low-temperature activity, while Fe-based catalyst presents more stable high-temperature performance. It is worth noting that both the two samples show nearly 40% of NO conversion at 125 °C, and less than 90% conversion could be obtained at 150 °C. For Cu(3.0)-Fe(1.3)-Beta, it is clear that the multiple metal-containing catalyst shows superior low-temperature activity. Cu(3.0)-Fe(1.3)-Beta appears similar performance with Fe(2.7)-Beta-4 catalyst at the high-temperature region. Moreover, the conversions of NH₃ on all catalysts are high above 200 °C, and the amount of N₂O yielded in the course of NH₃-SCR process is much less than 30 ppm. As a result, the bi-component Beta catalyst shows wider reaction-temperature window compared with the mono-component samples.

3.1.3. Activities in the presence of H₂O and SO₂

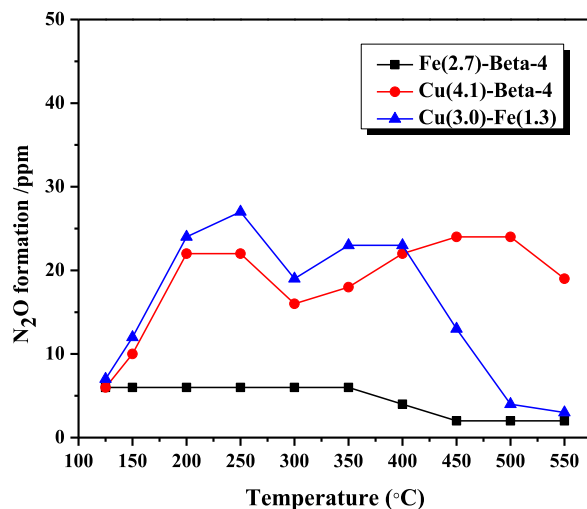
The catalytic performance of Al-rich Beta supported Cu, Fe catalysts in the presence of H₂O and SO₂ was studied, the results are shown in Fig. 3. When 2% H₂O and 100 ppm SO₂ was added to the reaction gas stream at 250 °C, it can be found that NO conversion



(a)



(b)



(c)

Fig. 2. SCR performance of the indicated catalysts. Reaction conditions: 500 ppm NO, 500 ppm NH₃, 10% O₂, and N₂ balance; GHSV: 80,000 h⁻¹.

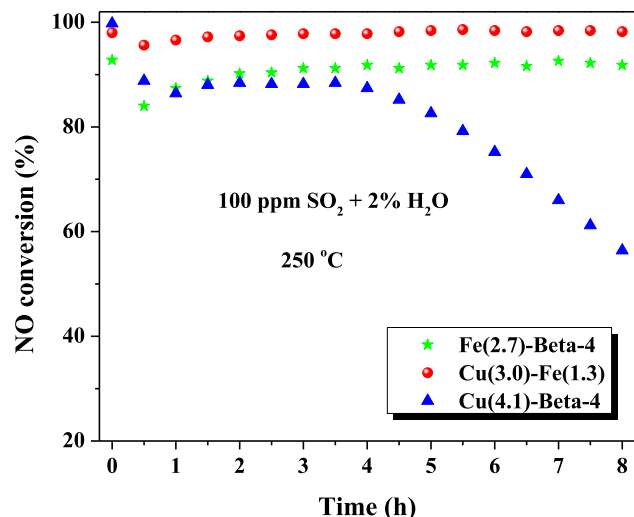


Fig. 3. The influences of H₂O and SO₂ on SCR activities of the indicated catalysts at 250 °C. Reaction conditions: 500 ppm NO, 500 ppm NH₃, 10% O₂, 2% H₂O, 100 ppm SO₂, and N₂ balance; GHSV: 80,000 h⁻¹.

for Cu(4.1)-Beta-4 decreased from 100 to 86% in 1 h (Fig. 3). At 1–4 h, NO conversion maintained at ca. 86%. After 4 h, however, NO conversion shows further decrease to ~50% at 8 h, demonstrating an unstable activity. For Fe(2.7)-Beta-4 catalyst, immediately after introduction of H₂O and SO₂, the activity in NO conversion decreases from ~93 to ~84% in 0.5 h. Interestingly, NO conversion then rapidly restores and maintains at ca. 90% in the residual reaction process. Cu(3.0)-Fe(1.3)-Beta presents the similar performance with Fe(2.7)-Beta-4 catalyst in the presence of H₂O and SO₂. After 8 h, NO conversion maintains at ~98%, which is a high level of activity. Thus, it can be found that Cu–Fe-bimetallic Beta catalyst shows better H₂O and SO₂ resistance compared with Cu- and Fe-monometallic Beta catalyst.

Furthermore, the hydrothermal stability of the catalysts against steaming is one of the most critical issues for the development of zeolite NH₃-SCR catalysts. Therefore, the hydrothermal stability of Cu(3.0)-Fe(1.3)-Beta catalyst was also evaluated. As shown in Fig. S2, after hydrothermal treatment with 10 vol% H₂O at 750 °C for 4 h, the Al-rich sample shows over 80% of NO conversion at the temperature region of 150–500 °C, indicating the better hydrothermal stability.

3.2. Characterizations on the fresh catalysts

Fig. 4 shows the XRD patterns of the single and multiple metal modified Beta catalysts. For Cu(4.1)-Beta-4 catalyst, it can be clearly detected the peaks of typical BEA structure. No obvious diffraction peaks of CuO crystallite appear, indicating that the active component would exist in the form of dispersed copper species. For Fe(2.7)-Beta-4 catalyst, it is clear that no pronounced diffraction peaks of α -Fe₂O₃ can be observed besides those of the Beta zeolite. It can be inferred that iron is dispersed on the Beta zeolite. For the Cu(3.0)-Fe(1.3)-Beta sample, it appears similar patterns with the above two samples. The existence of CuO and α -Fe₂O₃ crystallites could not be detected.

To obtain additional information on the active components of metals, the samples were studied by the UV–Vis–NIR characterization. As shown in Fig. 5, three obvious absorption bands could be detected for Cu(4.1)-Beta-4 centered at ~205 nm, ~286 nm and ~830 nm. According to the literature [14,15], the bands centered at

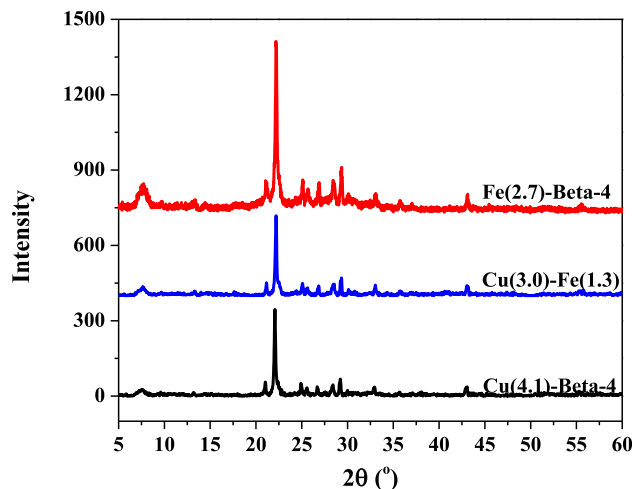


Fig. 4. XRD patterns of the indicated catalysts.

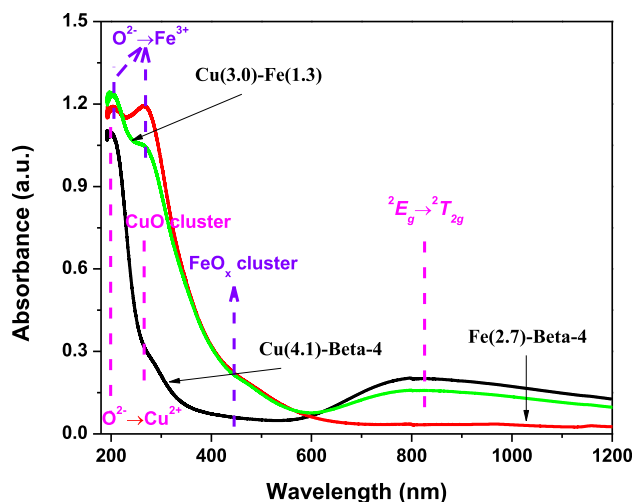


Fig. 5. UV–Vis–NIR spectra of the indicated catalysts.

205 nm and 830 nm can be attributed to the O²⁻ → Cu²⁺ charge transfer transitions, and the ²E_g → ²T_{2g} transition of Cu²⁺ ions in an octahedral environment, respectively, which are characteristic of the isolated Cu²⁺. The broad band at 280 nm may be attributed to the CuO cluster species. According to the intensity of relative bands, it can be inferred that the active component mainly exists in the form of isolated copper ions. For Fe(2.7)-Beta-4 catalyst, the spectrum shows three bands centered at ~208, ~270 and ~440 nm. The bands at 208 and 270 nm can be assigned to the charge transfer from O ligands to isolated Fe³⁺ in tetrahedral symmetry and octahedral symmetry, respectively [16,17]. Moreover, the band at 440 nm can be attributed to the FeO_x cluster species [16]. It is reasonable to suppose that isolated Fe³⁺ ions are the dominating species. For the Cu and Fe bi-component Beta catalyst, it appears four absorption bands centered at ~205, ~270, ~440 and ~830 nm, respectively, indicating the existence of isolated Cu²⁺, isolated Fe³⁺ and FeO_x cluster species despite of the overlapping signal of 205 nm. It is worthwhile to note that the bands of CuO and/or α -Fe₂O₃ crystallites could not be detected for all the samples. This is in good agreement with the XRD results.

Different copper and iron species were further characterized by EPR spectroscopy. As shown in Fig. 6, for Cu(4.1)-Beta-4 catalyst, a

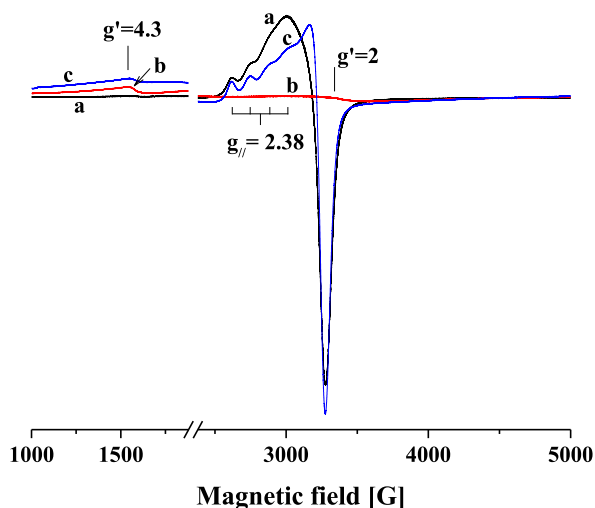


Fig. 6. EPR spectra of Cu(4.1)-Beta-4 (a), Fe(2.7)-Beta-4 (b) and Cu(3.0)-Fe(1.3)-Beta (c) catalysts at $-196\text{ }^{\circ}\text{C}$.

complex signal appears at $g_{\parallel} = 2.38$, $g_{\perp} = 2.07$, which is typical of isolated Cu^{2+} ions [18,19]. It is worthy to point out that probably due to the proximity of Cu^{2+} ions, the four splitting peaks ascribed to g_{\parallel} of isolated Cu^{2+} are difficult to discriminate. For Fe(2.7)-Beta-4 catalyst, the spectrum appears two signals at $g' \approx 4.3$ and $g' \approx 2$. According to the literature [20–22], the dominant signal at $g' \approx 4.3$ is characteristic of isolated tetrahedrally coordinated Fe^{3+} species in zeolites matrix, and the broad signal at $g' \approx 2$ may be attributed to the Fe^{3+} of FeO_x cluster, indicating the existence of isolated Fe^{3+} ions and FeO_x cluster species. These findings are consistent with the UV–Vis–NIR results. For both the bimetallic Beta catalysts, two signals appear in the spectra: one is a complex signal at $g_{\parallel} = 2.38$, $g_{\perp} = 2.07$ ascribed to the isolated Cu^{2+} ions, the other is centered at $g' \approx 4.3$ ascribed to the isolated tetrahedrally coordinated Fe^{3+} species in Beta. It is difficult to discriminate the signal of Fe^{3+} of FeO_x cluster due to the similar region with that of g_{\perp} of isolated Cu^{2+} ions. Comparing the EPR signal of isolated Cu^{2+} ions of Cu(3.0)-Fe(1.3)-Beta with that of Cu(4.1)-Beta-4, it is clear that the splitting peaks are more pronounced for bimetallic catalysts. This could be attributed to the increased distance of isolated Cu^{2+} ions, indicating the improvement of dispersion state. Actually, the dispersion state of copper and iron within the Beta crystal was studied by EDS. As can be seen in Fig. S3, Cu and Fe species were homogeneously dispersed.

XPS spectra of Cu 2p and Fe 2p bands of the samples are shown in Fig. 7. For Cu(4.1)-Beta-4 sample, the fittings of Cu 2p peaks were performed by two components, which present binding energy (BE) at 935.2 and 932.3 eV corresponding to surface Cu^{2+} and Cu^+ species, respectively [23,24]. The ratio of $\text{Cu}^{2+}/\text{Cu}^+$ is calculated by the area ratio of corresponding peaks. As shown in Table 1, the ratio of $\text{Cu}^{2+}/\text{Cu}^+$ on Cu(4.1)-Beta-4 is as low as 0.1, indicating that the surface active components mainly exist in the form of Cu^+ species. For bi-component Beta catalysts, the ratio of $\text{Cu}^{2+}/\text{Cu}^+$ increase to 0.28 over Cu(3.0)-Fe(1.3)-Beta. It can be inferred that the introduction of Fe increases the proportion of Cu^{2+} species. For Fe(2.7)-Beta-4 catalyst, the fitting peaks appear BE at about 713.3 and 709.7 eV corresponding to surface Fe^{3+} and Fe^{2+} species, respectively [25,26]. According to Table 1, the ratio of $\text{Fe}^{3+}/\text{Fe}^{2+}$ is about 0.96 for Fe(2.7)-Beta-4. While for Cu(3.0)-Fe(1.3)-Beta, the ratio is 1.85. It is clear that the proportion of Fe^{3+} species is higher on the Cu(3.0)-Fe(1.3)-Beta catalyst.

3.3. Characterizations on the used catalysts

To better understand the reason why SCR catalysts deactivated after sulfidation, the used Cu(4.1)-Beta-4 sample was studied by TGA coupled with TPD experiments. As can be seen in Fig. 8(A), the TG curve reveals three weight-loss stages. Accordingly, three obvious weight-loss peaks centered at 75, 419 and 655 $^{\circ}\text{C}$ appear in DTG profile. Combining the TPD results (Fig. 8(B)), one can believe that the first weight-loss peak at low temperature may be attributed to the desorption of adsorbed H_2O . At the middle-temperature region (250–550 $^{\circ}\text{C}$), the signals of formation of NH_3 , N_2 , SO_2 and H_2O can be detected, which is in good agreement with the products of $(\text{NH}_4)_2\text{SO}_4$ decomposition. It is necessary to assume that the decomposition of $(\text{NH}_4)_2\text{SO}_4$ is initiated by the release of NH_3 followed by that of other products. Thus, the formation of NH_3 can be first detected at 350 $^{\circ}\text{C}$. Actually, the weight-loss peak of 350 $^{\circ}\text{C}$ can also be observed in the DTG profile, which proves the assumption. Therefore, it can be inferred that the weight-loss at the middle-temperature region is attributed to the decomposition of deposited $(\text{NH}_4)_2\text{SO}_4$ species. Moreover, the weight-loss peak at ca. 655 $^{\circ}\text{C}$ may be attributed to the decomposition of deposited copper sulfates. Based on these results, it is reasonable to suggest that due to the continuous deposition of various sulfates formed during the reaction process, the SCR catalyst gradually lost its activity.

The sulfated Fe(2.7)-Beta-4 and Cu(3.0)-Fe(1.3)-Beta samples were also studied by the TGA method. It is clear that both samples show three obvious weight-loss peaks with an inconspicuous shoulder peak (Fig. 9), which are very similar with that of the sulfated Cu(4.1)-Beta-4 sample. As discussed above, three weight-loss stages can be attributed to the adsorbed H_2O , the deposited $(\text{NH}_4)_2\text{SO}_4$ species, the deposited iron sulfates and/or copper sulfates, respectively. It is worth noting that the deposited sulfates over Fe-containing Beta samples are less than that over Cu(4.1)-Beta-4 according to the intensity of corresponding weight-loss peaks.

4. Discussion

Cu(4.1)-Beta-4 catalyst shows high NO conversion below 300 $^{\circ}\text{C}$ compared with Fe(2.7)-Beta-4. After introduction of Fe, the Cu and Fe multiple metals containing Beta catalyst shows better low-temperature activity. Even at the temperature as low as 125 $^{\circ}\text{C}$, NO conversion can reach 85% over Cu(3.0)-Fe(1.3)-Beta. Meanwhile, the catalyst shows stable activity at the high-temperature region, which is very similar with Fe(2.7)-Beta-4. Combining the XRD and UV–Vis–NIR results, it is clear that the active components mainly exist in the form of isolated Cu^{2+} and Fe^{3+} ions, as well as small amount of CuO cluster and FeO_x cluster species. According to the EPR results, it can be found that the dispersion state of Cu^{2+} over bimetallic Beta catalysts is better than Cu(4.1)-Beta-4. This implies that the introduction of Fe is helpful to improve the dispersion state of copper. Based on the results of oxidation state study of the active components, it is demonstrated that the ratio of $\text{Cu}^{2+}/\text{Cu}^+$ and/or $\text{Fe}^{3+}/\text{Fe}^{2+}$ over Cu(3.0)-Fe(1.3)-Beta bi-component catalyst is higher than that over mono-component catalysts. Thus, Cu(3.0)-Fe(1.3)-Beta catalyst has the highest ratio of $\text{Cu}^{2+}/\text{Cu}^+$ and $\text{Fe}^{3+}/\text{Fe}^{2+}$. So, better dispersion state and higher concentration of Cu^{2+} and Fe^{3+} were achieved for Cu(3.0)-Fe(1.3)-Beta due to the synergistic effect of Cu and Fe. In terms of the best low-temperature activity that Cu(3.0)-Fe(1.3)-Beta has, it can be inferred that the isolated Cu^{2+} and Fe^{3+} located at the exchange sites may play a key role at the low-temperature region. On the other hand, Cu(3.0)-Fe(1.3)-Beta presents the identical performance with Fe(2.7)-Beta-4 at higher temperatures. Combining the UV–Vis–NIR results, it is found that the two samples appear similar intensity of

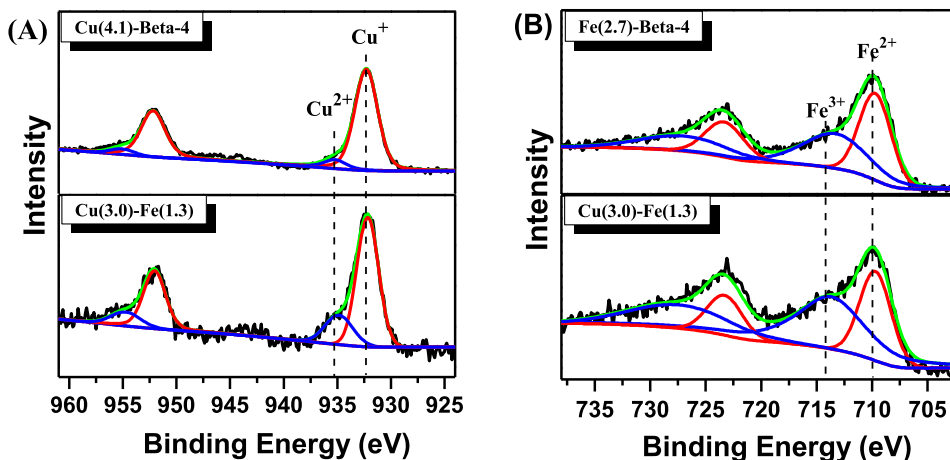


Fig. 7. XPS results of Cu 2p (A), and Fe 2p (B) in the indicated catalysts.

Table 1
XPS results of (A) Cu 2p, and (B) Fe 2p in the indicated catalysts.

Sample	Cu ²⁺	Cu ⁺	Cu ²⁺ /Cu ⁺	Fe ³⁺	Fe ²⁺	Fe ³⁺ /Fe ²⁺
Cu(4.1)-Beta-4	935.2	932.3	0.10	—	—	—
Fe(2.7)-Beta-4	—	—	—	713.3	709.7	0.96
Cu(3.0)-Fe(1.3)	935.0	932.2	0.28	713.5	709.7	1.85

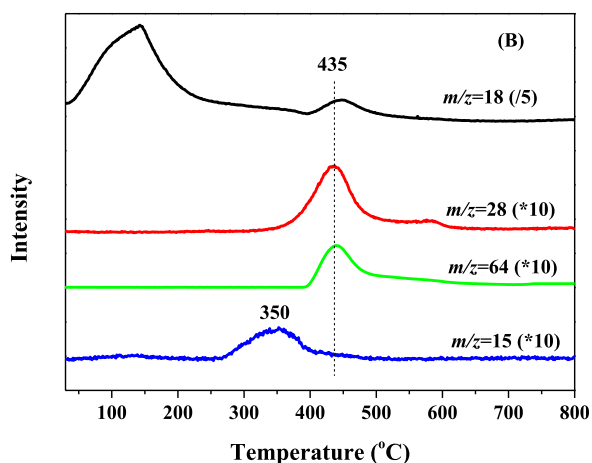
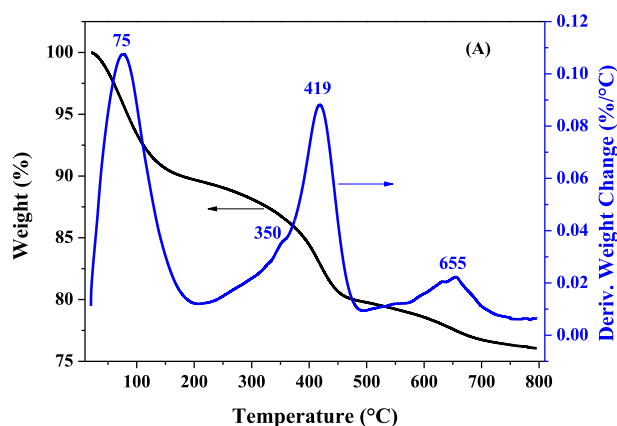


Fig. 8. TGA/DTG (A) and TPD (B) profiles of the sulfated Cu(4.1)-Beta-4 sample, temperature ramp rate: 10 °C/min.

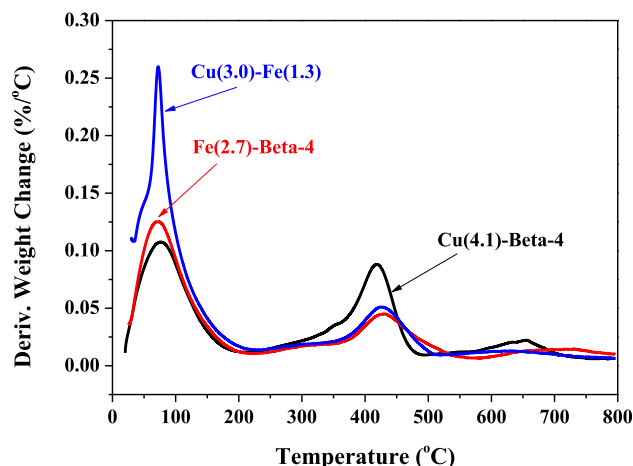


Fig. 9. DTG profiles of the sulfated Cu(4.1)-Beta-4, Fe(2.7)-Beta-4, and Cu(3.0)-Fe(1.3)-Beta samples, temperature ramp rate: 10 °C/min.

FeO_x clusters. Therefore, it is reasonable to suggest that FeO_x cluster species may contribute more to the high-temperature activity. The findings are consistent with the suggestion proposed by Brandenberger et al. [5]. Actually, with decrease of Fe concentration to lower level, Cu(4.0)-Fe(0.6)-Beta shows decreased high-temperature activity compared with other bi-component catalysts, which can further testify the suggestion.

After introduction of H₂O and SO₂ to the reaction system, Cu(4.1)-Beta-4 catalyst gradually loss its activity. While the Fe-containing Beta samples including Fe(2.7)-Beta-4 and Cu(3.0)-Fe(1.3)-Beta show the relative stable catalytic performance. By means of TGA and TPD methods, it can be found that the deposited sulfates may result in the deactivation of Cu(4.1)-Beta-4 catalyst. Comparing the intensity of the peaks towards the DTG profiles of the three samples, one can believe that sulfates may deposit more easily on the surface of Cu(4.1)-Beta-4. Thus, Fe(2.7)-Beta-4 and Cu(3.0)-Fe(1.3)-Beta catalysts show better activity in the presence of H₂O and SO₂. These results demonstrate that the deactivation is mainly caused by the (NH₄)₂SO₄ deposition at low temperature of 250 °C.

In summary, it can be concluded that with the introduction of Fe to the Cu-based Beta catalyst, improved dispersion state and increased Cu²⁺ and Fe³⁺ species are obtained. Due to these synergistic effects, Cu(3.0)-Fe(1.3)-Beta shows superior low-temperature

activity and wider activated temperature window as well as better H₂O and SO₂ resistance properties.

5. Conclusions

Copper and iron bimetallic Beta catalysts have been prepared and investigated for NH₃-SCR of NO. With the appropriate amount of Cu and Fe, Cu(3.0)-Fe(1.3)-Beta catalyst presents superior catalytic performance. NO conversion reaches 85% at the low temperature of 125 °C. Especially, over 80% of NO conversion is achieved at the wide temperature window of 125–500 °C. The combination of XRD, UV–Vis–NIR, EPR and XPS characterizations demonstrate the improvement of dispersion state of the active components and increase of surface Cu²⁺ and Fe³⁺ species caused by the synergistic effect of Cu and Fe. The isolated Cu²⁺ and Fe³⁺ ions at the exchange sites of Beta zeolite may account for the high activity at lower temperatures. On the other hand, FeO_x cluster species are helpful to the enhancement of high-temperature activity. Furthermore, Cu(3.0)-Fe(1.3)-Beta catalyst shows significant improvement of SO₂ resistance ability compared to Cu(4.1)-Beta-4. The easier deposition of ammonia sulfates on the latter is believed to be the reason of deactivation.

Acknowledgements

This work was supported by the INCOE (International Network of Centers of Excellence) project coordinated by BASF SE, Germany. W.Z. and C.S. thank the supports of the National Natural Science Foundation of China (No. 21373035, 21373037 and 21577013), the Fundamental Research Funds for the Central Universities (No. DUT13YQ107, DUT14RC(3)073, DUT16ZD224).

Appendix A. Supplementary data

Supplementary data related to this article can be found at <http://dx.doi.org/10.1016/j.micromeso.2016.08.042>.

References

- [1] J.H. Baik, S.D. Yim, I.S. Nam, Y.S. Mok, J.H. Lee, B.K. Cho, S.H. Oh, *Top. Catal.* 30–1 (2004) 37–41.
- [2] H. Sjövall, L. Olsson, E. Fridell, R.J. Blint, *Appl. Catal. B* 64 (2006) 180–188.
- [3] T. Komatsu, M. Nunokawa, I.S. Moon, T. Takahara, S. Namba, T. Yashima, *J. Catal.* 148 (1994) 427–437.
- [4] R.Q. Long, R.T. Yang, *J. Am. Chem. Soc.* 121 (1999) 5595–5596.
- [5] S. Brandenberger, O. Krocher, A. Tissler, R. Althoff, *Appl. Catal. B* 95 (2010) 348–357.
- [6] S. Brandenberger, O. Krocher, A. Tissler, R. Althoff, *Catal. Rev.* 50 (2008) 492–531.
- [7] A.V. Kucherov, D.E. Doronkin, A.Y. Stakheev, A.L. Kustov, M. Grill, *J. Mol. Catal. A* 325 (2010) 73–78.
- [8] P.S. Metkar, M.P. Harold, V. Balakotiah, *Appl. Catal. B* 111–112 (2012) 67–80.
- [9] A. Sultana, M. Sasaki, K. Suzuki, H. Hamada, *Catal. Commun.* 41 (2013) 21–25.
- [10] X. Yang, Z. Wu, M. Moses-Debusk, D.R. Mullins, S.M. Mahurin, R.A. Geiger, M. Kidder, C.K. Narula, *J. Phys. Chem. C* 116 (2012) 23322–23331.
- [11] L. Xu, C. Shi, Z. Zhang, H. Gies, F.-S. Xiao, D. De Vos, T. Yokoi, X. Bao, M. Feyen, S. Maurer, B. Yilmaz, U. Müller, W. Zhang, *Micropor. Mesopor. Mater.* 200 (2014) 304–310.
- [12] B. Xie, J.W. Song, L.M. Ren, Y.Y. Ji, J.X. Li, F.S. Xiao, *Chem. Mater.* 20 (2008) 4533–4535.
- [13] B. Yilmaz, U. Müller, M. Feyen, S. Maurer, H. Zhang, X. Meng, F.-S. Xiao, X. Bao, W. Zhang, H. Imai, T. Yokoi, T. Tatsumi, H. Gies, T. De Baerdemaeker, D. De Vos, *Catal. Sci. Tech.* 3 (2013) 2580–2586.
- [14] S. Kieger, G. Delahay, B. Coq, B. Neveu, *J. Catal.* 183 (1999) 267–280.
- [15] S.A. Yashnik, Z.R. Ismagilov, V.F. Anufriyenko, *Catal. Today* 110 (2005) 310–322.
- [16] M.S. Kumar, M. Schwidder, W. Grünert, A. Brückner, *J. Catal.* 227 (2004) 384–397.
- [17] P. Balle, B. Geiger, S. Kureti, *Appl. Catal. B* 85 (2009) 109–119.
- [18] P.J. Carl, S.C. Larsen, *J. Catal.* 182 (1999) 208–218.
- [19] F. Gao, E.D. Walter, E.M. Karp, J. Luo, R.G. Tonkyn, J.H. Kwak, J. Szanyi, C.H.F. Peden, *J. Catal.* 300 (2013) 20–29.
- [20] M. Schwidder, M. Santhosh Kumar, A. Bruckner, W. Grunert, *Chem. Commun.* (2005) 805–807.
- [21] M. Høj, M.J. Beier, J.-D. Grunwaldt, S. Dahl, *Appl. Catal. B* 93 (2009) 166–176.
- [22] D.E. Doronkin, A.Y. Stakheev, A.V. Kucherov, N.N. Tolkachev, G.O. Bragina, G.N. Baeva, P. Gabrielsson, I. Gekas, S. Dahl, *Mendeleev Commun.* 17 (2007) 309–310.
- [23] Z.C. Si, D. Weng, X.D. Wu, J. Li, G. Li, *J. Catal.* 271 (2010) 43–51.
- [24] N. Wilken, K. Wijayanti, K. Kamasamudram, N.W. Currier, R. Vedaiyan, A. Yezerets, L. Olsson, *Appl. Catal. B* 111 (2012) 58–66.
- [25] C. He, Y. Wang, Y. Cheng, C.K. Lambert, R.T. Yang, *Appl. Catal. A* 368 (2009) 121–126.
- [26] S. Shwan, R. Nedyalkova, J. Jansson, J. Korsgren, L. Olsson, M. Skoglundh, *Ind. Eng. Chem. Res.* 51 (2012) 12762–12772.